

Supporting Information  
for

Monitoring a reaction at sub-millisecond  
resolution in picoliter volumes

*Ansgar M. Huebner,<sup>†,#</sup> Chris Abell,<sup>#</sup> Wilhelm T. S. Huck,<sup>#</sup> Charles N. Baroud<sup>§,\*</sup> and  
Florian Hollfelder<sup>†,\*</sup>*

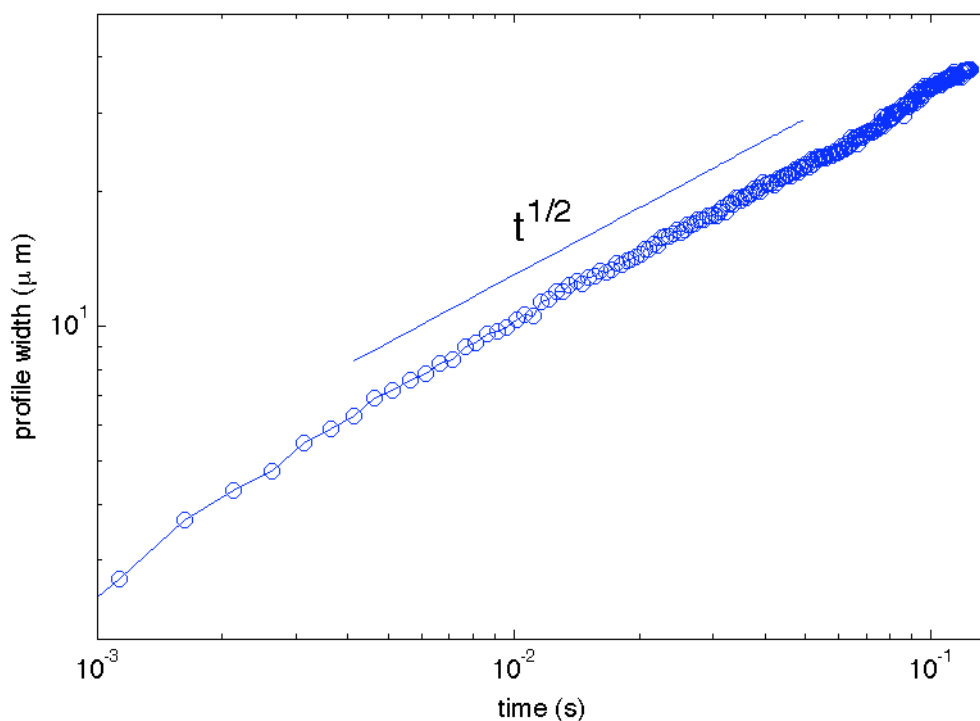
<sup>†</sup>Department of Biochemistry, University of Cambridge, Cambridge, CB2 1GA,  
United Kingdom.

<sup>#</sup>Department of Chemistry, University of Cambridge, Cambridge, CB2 1EW, United  
Kingdom

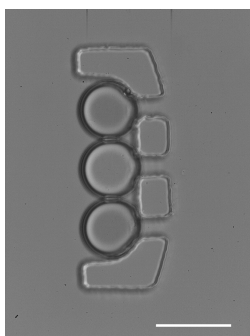
<sup>§</sup>Laboratoire d'Hydrodynamique (LadHyX) and Department of Mechanics, Ecole  
Polytechnique, F-91128 Palaiseau, Cedex, France

AUTHOR EMAIL ADDRESS: [baroud@ladhyx.polytechnique.fr](mailto:baroud@ladhyx.polytechnique.fr), [fh111@cam.ac.uk](mailto:fh111@cam.ac.uk)

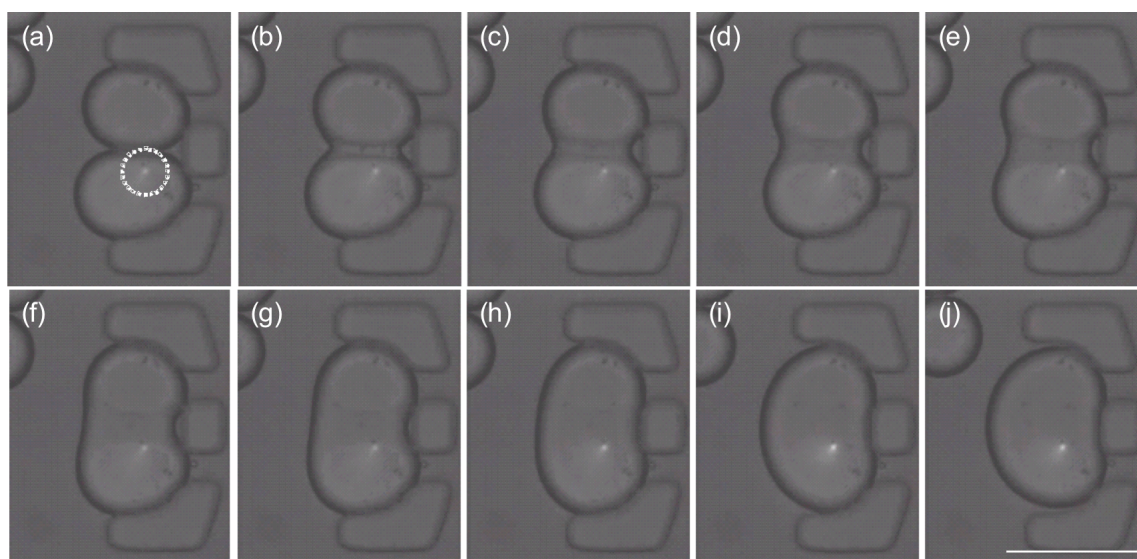
**(A) Supplementary Figures**



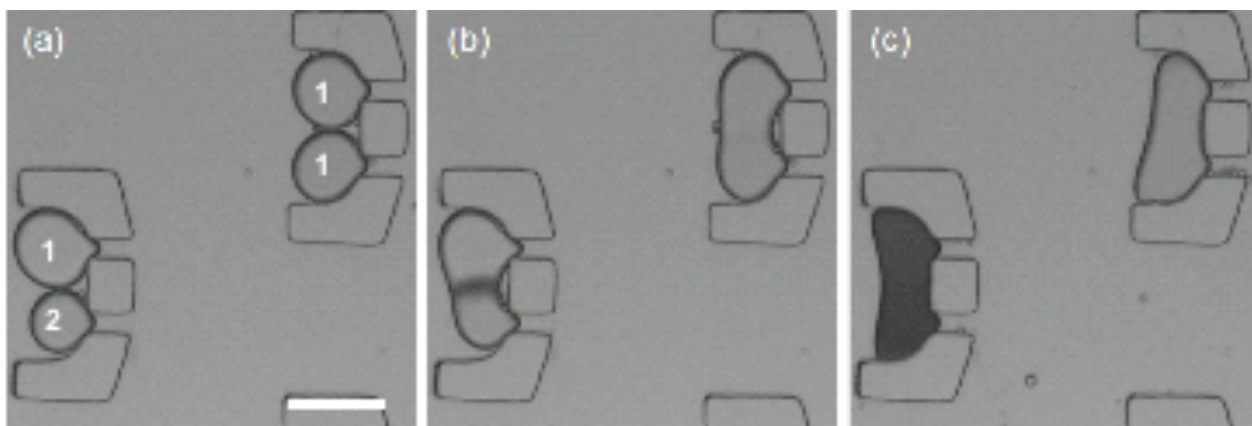
**Supplementary Figure S1:** Width of the experimentally measured concentration profile, shown on log-log axes. The  $t^{1/2}$  line is shown to guide the eye. Note the close agreement in slope, indicating that the profile width increases in a diffusive manner.



**Supplementary Figure S2:** Three droplets can be entrapped in a well that was designed analogously to the double wells discussed in the main text (Figure 1b). The design of the double trap (Figure 1B) was extended by the diameter of one droplet and an additional channel was added.



**Supplementary Figure S3: Laser-induced droplet fusion.** (a) Two trapped droplets filled with an aqueous phase with fluorescent dye (100 mM FITC, in phosphate buffered saline, pH 7.4). The laser beam (Piccaro 488 nm air-cooled cyan) is denoted by a white circle and made visible by the fluorophore dissolved in the aqueous phase. As a consequence of heat absorption by the fluorophore, the droplets temperature increases locally triggering fusion as a consequence of local depletion of the surfactant. Pictures were taken at different time points, i.e. (a) 0  $\mu$ s, (b) 500  $\mu$ s, (c) 1 ms, (d) 1.5 ms, (e) 2 ms, (f) 5 ms, (g) 19 ms, (h) 72 ms, (i) 170 ms and (j) 350 ms, using a fast-camera (V7.2, Phantom) mounted onto a microscope (IX 71, Olympus). A scale bar corresponding to 75  $\mu$ m is shown in image (j). Temperature:  $24 \pm 1.5$  °C.



**Supplementary Figure S4: Simultaneous fusion of two different droplet pairs.** The image shows two traps, each containing a different combination of droplets (indicated with numbers 1 = KSCN and 2 =  $\text{Fe}(\text{NO}_3)_3$ ). (a) Two different droplets are immobilized (b) Electro-coalescence leads to joining of both droplet pairs and formation of the complex in one of them. Images were taken with a fast camera (V7.2, Phantom) mounted onto a microscope (IX 71, Olympus). A scale bar corresponding to  $75 \mu\text{m}$  is shown in image (a).

# Derivation of the reaction-diffusion system of equations

## B1 - Theoretical formulation

Consider the complexation reaction between  $Fe^{3+}$  and  $SCN^-$  and suppose that the reaction is irreversible. For shorthand we will denote A the  $Fe^{3+}$  ions and B the  $SCN^-$  ions, which give C, the  $Fe(SCN^-)_3$  complex. The stoichiometry of the reaction is<sup>1</sup>



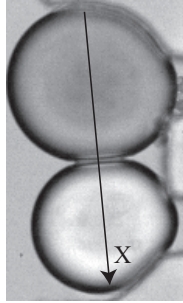
The depletion of A and B and the creation of C are limited by the total rate of the reaction  $k$  and by the diffusion of the three species, whose diffusion coefficients we write  $D_{a,b,c}$ . The concentrations  $A, B$  and  $C$  of the three species can therefore vary in space and in time  $A(X, T)$ , etc. and we can write the following reaction-diffusion equations [1]:

$$\frac{\partial A}{\partial T} = D_a \frac{\partial^2 A}{\partial X^2} - kAB^3, \quad (2)$$

$$\frac{\partial B}{\partial T} = D_b \frac{\partial^2 B}{\partial X^2} - 3kAB^3, \quad (3)$$

$$\frac{\partial C}{\partial T} = D_c \frac{\partial^2 C}{\partial X^2} + kAB^3. \quad (4)$$

Here,  $A, B, C$  denote the concentrations of the three species (in mol/L),  $T$  is the time and  $X$  is the spatial direction transverse to the initial droplet separation. This gives units of  $(L/mol)^3 s^{-1}$  for  $k$ .



**Supplementary Figure S5:** Definition of the  $X$  direction on the initial image, at  $T = 0$ .

We would like to non-dimensionalize this system of equations in order to obtain a general solution. For this we will use:

$$\chi = \sqrt{\frac{D_a}{D_b}}, \quad (5)$$

$$\beta = \sqrt{\frac{A_0}{B_0}}, \quad (6)$$

where  $A_0$  and  $B_0$  are the initial concentrations of A and B, respectively. For the spatial and time scales we use:

---

<sup>1</sup>A stoichiometry of  $A + B \rightarrow C$  was also tested and yielded unsatisfactory results, suggesting that the stoichiometry in Eq. 1 is the correct one.

$$L^2 = \frac{\sqrt{D_a D_b}}{k A_0 B_0^2}, \quad (7)$$

and

$$\tau = \frac{1}{k A_0 B_0^2}. \quad (8)$$

We can now define  $a = A/A_0$ ,  $b = B/B_0$  and  $c = C/\sqrt{A_0 B_0}$ ,  $x = X/L$  and  $t = T/\tau$ , giving the dimensionless variables which are written using lower case symbols. Also, we can suppose that  $D_c \simeq D_a$  since the two iron ions will diffuse at similar rates, thus reducing the number of parameters by one. Plugging in these forms into Eqs. 2-4, we obtain the dimensionless form of the reaction-diffusion problem:

$$\frac{\partial a}{\partial t} = \chi \frac{\partial^2 a}{\partial x^2} - \frac{1}{\beta^2} ab^3, \quad (9)$$

$$\frac{\partial b}{\partial t} = \frac{1}{\chi} \frac{\partial^2 b}{\partial x^2} - 3ab^3, \quad (10)$$

$$\frac{\partial c}{\partial t} = \chi \frac{\partial^2 c}{\partial x^2} + \frac{1}{\beta} ab^3. \quad (11)$$

Note that the reaction rate does not enter into the non-dimensionalized problem anymore and this system of equations can be solved in the general case, which is valid for any value of  $k$ . The comparison between the numerical solution and the experimentally measured production of the reaction product  $C$  can then yield the fitting parameter  $\tau$  which, combined with knowledge of the initial concentrations  $A_0$  and  $B_0$ , yields  $k$ .

## B2 - Numerical solution

These equations can be solved in matlab using the `pdepe.m` function, and using the initial conditions given from the experiment, namely  $A_0 = 0.27 \times 10^{-3}$  and  $B_0 = 0.8 \times 10^{-3}$  mol/m<sup>3</sup>. The values of the diffusion coefficients were obtained from Ref. [2]:  $D_a \simeq D_c = 0.72 \times 10^{-9}$  m<sup>2</sup>/s and  $D_b = 1.76 \times 10^{-9}$  m<sup>2</sup>/s.

Figure shows the concentrations of the three species at two characteristic moments of the simulation. While A and B begin with a sharp interface, the species initially rapidly inter-diffuse and react together, followed by a slowing down of the spread of the overlap zone. We therefore initially see a rapid increase in the concentration of C but that increase slows down as the time required to diffuse A and B becomes large, thus ‘‘diffusion limiting’’ the reaction.

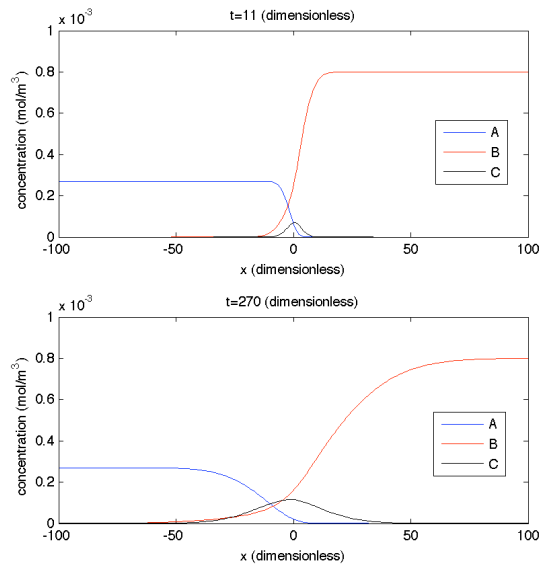
The comparison between the experiment and simulation can be made globally, by plotting the spatio-temporal field of concentration  $c$  vs. the gray scale values obtained from the experiments, as shown in Fig. .

$k$  enters into the system in two ways: In  $\tau$  and in  $L^2$  (Eqs. 8 and 7). Therefore choosing a value of  $k$  will stretch the horizontal and vertical axes on the numerical part of Fig. .

## B3 - Fitting the experiments and simulations

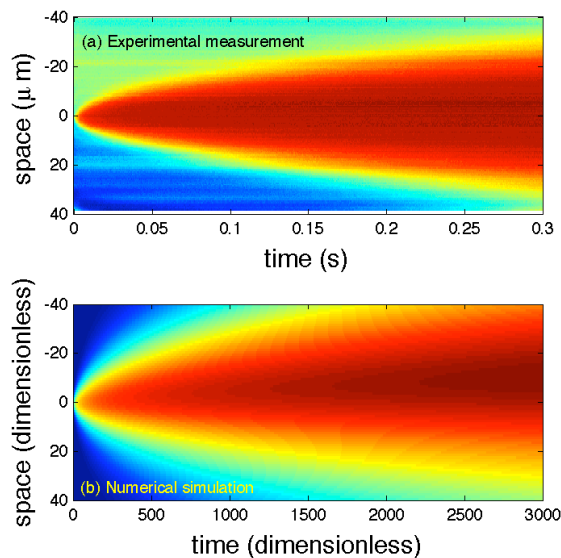
In fitting the experimental and numerical data, two parameters must be chosen.

### Gray value calibration



**Supplementary Figure S6:** Concentrations of the reagents and the reaction product at two different dimensionless times.

The first gives the relation between the gray value and the concentration of the reaction product. In the absence of independent calibration of the gray value vs  $C$ , the correspondence was obtained by comparing the width of the numerical and experimental curves as a function of time. Indeed, the linearity of the correspondence between gray value and product concentration is best at low concentrations, a situation which occurs both at the early times of the reaction and near the edge of the reaction zone.

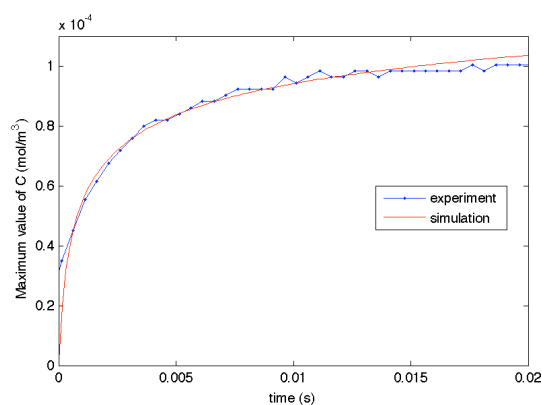


**Supplementary Figure S7:** Concentration field of reaction product  $c$  as a function of space and time, comparison between simulated and measured fields.

Therefore by comparing the broadening of the reaction zone as a function of time between experiments and simulations, a best fit of 27 gray value counts for a numerically calculated concentration of  $C = 10^{-4} \text{ mol/m}^3$  can be obtained.

### Reaction rate

Once the gray value correspondence is chosen, the reaction rate can be obtained by comparing the numerically calculated production of  $c$  with the measured increase. A fit of the measured and simulated value over the first 20 ms yields  $\tau = 0.2 \text{ ms}$  or equivalently  $k = 3 \times 10^4 \text{ M}^{-3}\text{s}^{-1}$ . The correspondence between the experiments and simulations is shown in Fig. .



**Supplementary Figure S8:** Maximum value of the concentration as a function of time, given in dimensional variables for a fitting value  $\tau = 0.2 \text{ ms}$ .



# Bibliography

- [1] P. M. J. Trevelyan, D. E. Strier, and A. De Wit. Analytical asymptotic solutions of  $nA + mB \rightarrow C$  reaction-diffusion equations in two-layer systems: A general study. *Phys. Rev. E (Statistical, Nonlinear, and Soft Matter Physics)*, 78(2):026122, 2008.
- [2] Lide, editor. *CRC Handbook of Chemistry and Physics*. CRC Press, 2004.